

<b>TRIUMF</b>	<b>UNIVERSITY OF ALBERTA EDMONTON, ALBERTA</b>	
	Date 2007/06/25	File No. TRI-DNA-07-1
Authors D Evans, D Louie, K Reiniger and GM Stinson	Page 1 of 22	

*Subject* Further measurements of the properties of the ANAC ac steering magnets

## 1. Introduction

It is proposed to insert ac steering magnets into beam line 2A between the  $\pm 15^\circ$  switching magnet and each of the downstream  $15^\circ$  dipoles. Their purpose is to allow rastering of the beam on each of the east and west targets. Previous studies<sup>1)</sup> have indicated that use of the ANAC ac steerers that were obtained from the University of Alberta could produce an annular beam spot with a central radius of  $\sim 7$  mm at the targets provided that they were operated at a frequency of 20 Hz or less. The cut-off frequency is determined by the frequency responses of the steerers.

The performance of these magnets was measured previously under dc conditions<sup>2)</sup> and the measurements were found to agree with the specifications given by the manufacturer. These are listed below.

---

Aperture diameter	3.04 inches	Maximum field	0.13 kG
Vacuum chamber clearance diameter	2.60 inches	Maximum power	15 V, 3.5 A
Overall diameter	8.00 inches	Unipolar power supply	15 V, 3.5 A
Overall length	11.65 inches	Bipolar power supply	$\pm 36$ V, 5 A
Effective length	11.52 inches	Inductance	0.032 H

---

This report continues the study of these magnets under ac conditions.

## 2. Measurements

For these measurements a Bell 615 Gauss meter with a transverse probe was used to measure  $B_{rms}$ . With its function switch on AC this instrument indicates  $B_{rms}$  on its front panel. An oscilloscope calibrated to  $100 \text{ mV} = 100 \text{ G}$  was used to measure  $B_{peak}$  for some of the runs. A KEPCO power supply capable of producing a voltage of 100 V peak-to-peak at 3.5 A was used to drive the steering magnets.

The first measurements were made in late March on the vertical coil of magnet #14.  $B_{peak}-I_{rms}$  and  $B_{rms}-I_{rms}$  curves were taken for (ac) currents from 0.5 A to 3.5 A in 0.5 A steps. The upper limit of the current was set by the specifications of the magnet. For each current the dc and rms ac fields and voltages from the gauss meter and the peak fields observed on the oscilloscope were recorded.

A second set of measurements were made in early May. In these runs  $B-I$  responses of the rms field and voltage were made for *each* of the horizontal and vertical coils of *each* of the four steering magnets. The frequency response from 7 Hz to 24 Hz was also made for two of the magnets. For the horizontal coil of one magnet a heating test over an eight-hour period was conducted at frequencies of 10 Hz and 20 Hz and at a current of 3.5 A rms. Finally, a scan was made along the center-line of a magnet.

Later in May, a complete mid-plane scan was made for one magnet. A frequency response curve to the limit of the power supply was also taken.

## 3. Results

### 3.1 Results of the first measurements

Although both coils were powered, dc and rms fields and voltages and peak fields were recorded only for the vertical coil of magnet #14. The results obtained are listed in Table 1.

For the reason discussed below, it is useful in analyzing the data from other runs to obtain the relationship between the  $B_{peak}$  and the  $B_{rms}$  data for this coil. Figure 1 is a plot of these measured values as a function of current.

Linear fits in current were made to each of these measured fields using the program PHYSICA<sup>3)</sup>. Also shown in figure 1 is  $B_{peak,fit}$  versus  $I_{rms}$ , the linear fit to the measured  $B_{peak}-I_{rms}$  data, and a plot of  $B_{peak,calc} = \sqrt{2} B_{rms,meas}$  versus  $I_{rms}$ , the expected variation of  $B_{peak}$  with respect to  $B_{rms}$ .

Explicitly, the linear relationships between  $B_{peak,meas}$  and  $B_{rms,meas}$  versus  $I_{rms}$  were found to be

$$B_{peak,meas}(\text{G}) = 54.642857 I_{rms}(\text{A}) - 0.285143$$

and

$$B_{rms,meas}(\text{G}) = 38.592857 I_{rms}(\text{A}) - 1.157143 ,$$

and that between  $B_{peak,meas}$  and  $B_{rms,meas}$  was found to be

$$B_{peak,meas}(\text{G}) = 1.415582 B_{rms,meas}(\text{G}) + 1.375347 .$$

The latter is very close to the expected value of  $B_{peak,meas} = \sqrt{2} B_{rms,meas} = 1.414214 B_{rms,meas}$ , albeit there is an offset of  $\sim 1.4$  G). Assuming that the offset of  $B_{peak,meas}$  from  $B_{rms,meas}$  would be approximately the same for the other coil of this magnet and those of the other three magnets, the error in calculating  $B_{peak}$  from  $B_{peak} = \sqrt{2} B_{rms}$  would be  $\sim 1.1\%$  at the value of  $B_{rms}$  expected to be used ( $\sim 100$  G).

From this we infer that from a measurement of  $B_{rms}$  one may obtain the value of  $B_{peak}$  using this reduced relationship ( $B_{peak} = \sqrt{2} B_{rms,meas}$ ).

### 3.2 Results from the second set of measurements

Because field maps were requested, all magnets and one power supply were moved from the power supply work area to the magnetic measurements survey table in the Proton Hall annex. Further, because of the automated nature of the measurements there, it was impractical to observe the  $B_{peak}$  values on the oscilloscope. It is for this reason that the relationship between  $B_{peak,meas}$  and  $B_{rms,meas}$  was necessary. The results (at least for one coil), as noted in §3.1, indicated that a measurement of  $B_{rms}$  was sufficient to determine  $B_{peak}$ .

Unless otherwise stated, all  $B_{rms}-I_{rms}$  tests were made with the probe in the center of the magnet; for these the maximum current was  $I_{rms} = 3.5$  A. All field maps were made at a current of  $I_{rms} = 3.5$  A. Except for the frequency-response tests, most measurements were made at 10 Hz; for the magnet-heating test, frequencies of 10 Hz and 20 Hz were used.

#### 3.2.1 Results of the complete set of B-I measurements

The magnet terminals marked 'H' are for horizontal steering and produce a vertical field component. Those marked 'V' are for vertical steering and produce a horizontal field component. All measurements were taken with *either* the horizontal *or* the vertical coil excited. *No* measurements were taken with currents flowing simultaneously in *both* coils.

Measurements of  $B_{rms}$  and  $V_{rms}$  as a function of  $I_{rms}$  were taken for each coil of each magnet. Data obtained from these measurements are given in tables 2 through 5.

From these tables we note that for all currents, magnet #9 requires an rms voltage for each coil that is approximately 10% higher than that required for the corresponding coils of magnets #11, #13 and #14. However, there is no significant difference from magnet to magnet in the field produced at a given current. This is in agreement with the results obtained from the dc measurements.

The power supplies that have been purchased for these magnets produce a maximum peak-to-peak voltage

of 100 V. This indicates a maximum rms voltage of  $50\text{ V}/\sqrt{2} = 35.36\text{ V}$  is attainable. Because two steerers are to be powered in series (and assuming the steerers to be identical), the maximum rms voltage per steerer would be  $17.68\text{ V}_{rms}$ . This poses no problem if the steerers are operated at a frequency of 10 Hz as in these tests, but there could be a problem were a higher frequency required.

A linear fit to the  $B_{rms,meas}-I_{rms}$  data presented in tables 2–5 was made. Assuming a fit of the form

$$B_{rms,meas}(\text{G}) = \alpha I_{rms}(\text{A}) + \beta ,$$

the coefficients for  $\alpha$  and  $\beta$  obtained for each coil of each magnet are listed in table 6.

Note that only the data given in tables 2 through 5 were used—that is, there was no attempt to force the fit through the origin  $(B_{rms}, I_{rms}) = (0, 0)$  either by adding a dummy point of that value or by deleting the constant term  $\beta$ .

A fit was also made to the total combined data. Again, no attempt was made to force the fit through  $(B_{rms}, I_{rms}) = (0, 0)$ . In this case we find that the  $B_{rms,meas}-I_{rms}$  relationship in the plane of vertical steering is given by

$$B_{vert,rms,meas}(\text{G}) = 39.1607143 I_{rms}(\text{A}) - 2.46071429 ,$$

and that in the plane of horizontal steering by

$$B_{hor,rms,meas}(\text{G}) = 39.1375 I_{rms}(\text{A}) - 2.475 .$$

It is interesting to note that in the horizontal plane the  $B_{hor,rms,meas}-I_{rms}$  fit to the entire set of measured data yields exactly the same  $\alpha$  and  $\beta$  values that are obtained by averaging the values for the fits to the individual horizontal plane measurements. In the vertical plane average value of  $\alpha$ , 39.1716071 G/A, differs from that of a fit to overall data, 39.1607143 G/A, by  $\sim 0.03\%$  whereas the average value of  $\beta$ ,  $-2.40671428\text{ G}$ , differs from that of a fit to overall data,  $-2.475$ , by  $\sim 2.2\%$ . From these results we suggest that the fits to the overall data in each plane are sufficient for use in calculations for  $B_{rms}$  given  $I_{rms}$  and hence  $B_{peak}$  from a given  $B_{rms}$ .

That this is so is indicated in tables 7 and 8, which show measured and fitted values of  $B_{rms}$  versus  $I_{rms}$ . The values for  $B_{rms,fit}$  were calculated using the above fits of the overall data for each of the vertical and horizontal planes. In these two tables the quantity  $B_{rms,diff}$  is defined as

$$B_{rms,diff} = 100 \frac{(B_{meas} - B_{calc,rms})}{B_{meas}}$$

where  $B_{meas}$  is the appropriate measured rms field.

Because we are interested in  $B_{rms}$  greater than 100 G, it is seen that the differences between measured and fitted values are less than 0.5%.

### 3.2.2 Frequency response

The manufacturer's data includes a plot of normalized field (at constant input voltage) of a magnet against frequency; the corner frequency is stated as 20 Hz. This plot is virtually flat at a value of unity from dc to 5 Hz, at which point the response begins to drop off. The normalized response is approximately 0.9 at 10 Hz, 0.8 at 15 Hz, 0.7 at 20 Hz, 0.6 at 26 Hz and 0.5 at 35 Hz. The remainder of the response curve is completed by drawing a straight line (on the log-log plot) through a normalized field of 0.25 at 80 Hz and one of 0.035 at 600 Hz. The implication of this response curve is that these magnets cannot be operated at TRIUMF at frequencies much above 10–20 Hz.

Because operation for some targets at a frequency in the order of 110 Hz has been suggested, it was decided to observe the frequency response of two of the steerers at *constant* current. A controller to drive the power supply at frequencies from 7 Hz to 24 Hz was provided by D. Louie. Frequency-response curves were taken

on both coils of magnets #9 and #13. These two magnets were chosen because the former required a higher supply voltage at the lower 10 Hz frequency than the latter and the other two magnets.

Measurements were taken at a current of 3.5 A rms with the probe located at the magnet center. Data taken are listed in tables 9 and 10; this data is plotted in figures 3 and 4 in which  $B_{rms,vert}$  and  $B_{rms,hor}$  are the measured values of the vertical and horizontal fields respectively.  $B_{rms,hor}$  was not recorded for magnet #13 because, as shown in table 9 and figure 2, its value did not change with frequency.

From both tables 9 and 10 and figures 2 and 3 it is clear that the required power supply voltage increases with frequency. This is because the inductive reactance is increasing with frequency and becoming larger than the resistive component. It is interesting that the two coils of either magnet differ in their voltage requirements. As the frequency increases the vertical coil of magnet #9 requires a higher voltage than its horizontal coil; the situation is reversed with magnet #13. However, although magnet #9 shows a  $\sim 2 V_{rms}$  offset relative to that required for magnet #13 at low (10 Hz) frequency, the voltages required for both magnets is approximately equal at a frequency of 20–24 Hz.

The measured magnetic fields appear to be almost frequency independent. If anything, they show a slight decreasing trend with increasing frequency.

Although part of the third set of measurements it seems logical to insert here the results of the extended frequency-response measurements that were made later on magnet #13. In this case the vertical and horizontal coils were independently connected to the full output of the power supply and their response over a frequency range from 20 Hz to 56 Hz was measured. The results are given in table 11.

In these measurements the sine-wave output from the power supply began to clip (flat top) at  $\sim 36.5 V_{rms}$ . This corresponds to a peak-to-peak voltage of  $2 \times \sqrt{2}(36.5) = 103 V$ , the rated output of the supply. At this point the measurements were stopped in order not to damage the power supply.

Figure 4 is a composite plot that includes both the frequency-response measurements for  $7 \text{ Hz} \leq f \leq 25 \text{ Hz}$  and  $20 \text{ Hz} \leq f \leq 54 \text{ Hz}$ . It is seen that the two sets of data overlap nicely.

### 3.2.3 Frequency response at higher frequencies

It seems reasonable to attempt to estimate what driving voltage would be required to operate these magnets at frequencies  $\sim 100$ – $110$  Hz. After consideration of the results shown in figure 4 one might be tempted to fit the measured data to a quadratic polynomial in frequency and use that function to predict the voltages at higher frequencies. This, however, would be incorrect as is shown below.

We assume that the magnet can be represented by a lumped- $R$ –lumped- $L$  series system. A power supply provides the magnet with an ac current given by

$$I = I_{peak} \sin(\omega t) = \sqrt{2} I_{rms} \sin(\omega t)$$

with  $\omega = 2\pi f = 2\pi/T$ ,  $f$  the frequency and  $T = 1/f$  the period of the provided current. Then the total voltage  $V$  across the R–L system is the sum of the voltage across the resistive element  $V_R$  and that across the inductive element  $V_L$ :

$$\begin{aligned} V &= V_R + V_L \\ &= R I_{peak} \sin(\omega t) + L \frac{dI}{dt} \\ &= R I_{peak} \sin(\omega t) + \omega L I_{peak} \cos(\omega t) \\ &= I_{peak} [X_R \sin(\omega t) + X_L \cos(\omega t)] , \end{aligned}$$

where we have written  $X_R = R$ , the resistance of the coil, and  $X_L = \omega L$ , its inductive reactance. Then

the value of  $V_{rms}$  is calculated from

$$V_{rms} = \sqrt{\int_0^T \frac{1}{T} V^2 dt} .$$

Because

$$V^2 = I_{peak}^2 [X_R \sin(\omega t) + X_L \cos(\omega t)]^2 = I_{peak}^2 [X_R^2 \sin^2(\omega t) + 2 X_R X_L \sin(\omega t) \cos(\omega t) + X_L^2 \cos^2(\omega t)] ,$$

we require the following integrations:

$$\int_0^T \sin^2(\omega t) dt = \int_0^T \frac{1 - \cos(2\omega t)}{2} dt = \frac{t}{2} \Big|_0^T - \frac{1}{4\omega} \sin(4\pi t/T) \Big|_0^T = \frac{T}{2} ,$$

$$\int_0^T \cos^2(\omega t) dt = \int_0^T \frac{1 + \cos(2\omega t)}{2} dt = \frac{t}{2} \Big|_0^T + \frac{1}{4\omega} \sin(4\pi t/T) \Big|_0^T = \frac{T}{2} ,$$

$$\int_0^T \sin(\omega t) \cos(\omega t) dt = \frac{\sin^2(\omega t)}{2\omega} \Big|_0^T = \frac{1}{2\omega} [\sin^2(2\pi T/T) - \sin^2(0)] = 0 .$$

Thus,

$$\begin{aligned} V_{rms}^2 &= \int_0^T \frac{1}{T} V^2 dt \\ &= \frac{I_{peak}^2}{2} [X_R^2 + X_L^2] \end{aligned}$$

or

$$V_{rms} = \frac{I_{peak}}{\sqrt{2}} \sqrt{X_R^2 + X_L^2} = I_{rms} \sqrt{X_R^2 + X_L^2}$$

This expression was used to calculate the frequency response expected for a (constant) value of  $I_{rms} = 3.5$  A. The values of  $R$  and  $L$  were varied in an attempt to fit the measured frequency response. Figure 4 shows the results of a fit using  $R = 3.5 \Omega$  and  $L = 0.0288$  Henry. Also plotted are the measured values  $V_{rms,meas}$  for the two frequency ranges  $7 \text{ Hz} \leq f \leq 25 \text{ Hz}$  and  $20 \text{ Hz} \leq f \leq 56 \text{ Hz}$ . The measured and calculated values of  $V_{rms}$  are seen to agree well. For reference purposes, we show in figure 5 the voltage waveforms across the resistive component, the inductive component and their sum over one period at 10 Hz.

One certainly may obtain equivalent fits to the data by adjusting the values of  $R$  and  $L$ . However, to fit the data these values do not vary by more than 10%. The selected value of  $R$  is more-or-less midway between the value calculated from the data in table 1 ( $\sim 3.35 \Omega$ ) and that given in the recent supplement to the TRIUMF Magnet Index ( $\sim 3.86 \Omega$ ). Further, the fitted value of  $L$  (29 mH) is in good agreement with the value quoted in the manufacturer's literature (32 mH).

Independently, two of us (DL and KR) simulated a magnet using values of  $R = 3.86 \Omega$  and  $L = 0.016$  Henry. Their simulation was carried out over a frequency range from dc to 10 kHz. Although they did not attempt to reproduce the measured data, they found a frequency-response curve similar to that of shown in figure 4. However, their results do not imply that the magnet could be operated at a frequency of 10 kHz.

As noted in §3.2.2, the manufacturer's data shows a frequency response that has a knee at  $\sim 20$  Hz. Our data shows no such knee; the measured field was essentially constant up to the maximum frequency ( $\sim 50$  Hz) at which the power supply did not clip. There was no indication that there would be problems at higher frequencies were the appropriate power supply available. We assume that these different frequency responses result from that of the manufacturer being taken at constant voltage input whereas ours was taken at constant current input.

### 3.2.4 Heating tests

Because it is expected that these (air-cooled) magnets would operate continuously for long periods of time, resistive heating will heat their coils and the resistances of the coils will increase. This will be observed as an increase in the driving voltage required for a given current. This phenomenon was measured using the horizontal (field) coil of magnet #13. The coil was run for 8 hours at a current of  $3.5 A_{rms}$  at frequencies of 10 Hz and 20 Hz. Voltage measurements were taken hourly. Actual temperature measurements were made only at the start and end of each test. The results of these measurements are given in table 12.

The increase in the required voltage because of increased coil resistance is  $\sim 6\%$  after the magnet had been running for eight hours at an rms current of 3.5 A and a frequency of 10 Hz. After running for the same time and current at a frequency of 20 Hz the voltage increase was  $\sim 3\%$ . After a longer running period a further voltage increase might be expected, but the total increase would be expected to be below 10%.

The measured temperature of the horizontal coil was  $22.0^\circ\text{C}$  at the beginning of the test and  $40.5^\circ\text{C}$  at the end. Corresponding temperatures when the coil was operated at 20 Hz were  $21.3^\circ\text{C}$  and  $40.0^\circ\text{C}$ . Thus the temperature increase of the coil was approximately  $20.0^\circ\text{C}$  at either frequency after running eight hours at 3.5 A rms. a further temperature increase would be expected after a longer running period, but that increase would be expected to be no more than  $5^\circ\text{C}$ .

Consequently, we feel that heating of the coil over a long running period should not pose a problem.

### 3.2.5 Field measurements along the central axis of magnet #9

Measurements of the (rms) vertical and horizontal fields along the axis of magnet #9 were made at an rms current of 3.5 A and a frequency of 10 Hz. Data taken in this measurement are listed in table 13. Figures 6(a) and 6(b) show the rms fields along the axis of the magnet in the vertical and horizontal planes respectively.

No further analysis of these data is undertaken here because of the mid-plane measurements detailed in the section below.

### 3.3 Mid-plane measurements of magnet #13

The final measurement was a mid-plane mapping of the vertical (rms) field of magnet #13 at a current of  $I_{rms} = 3.5 \text{ A}$  and a frequency of  $f = 10 \text{ Hz}$ . Measurements were made for longitudinal coordinates ( $z$ ) over the range of  $-10 \text{ in.} \leq z \leq 10 \text{ in.}$  and transverse coordinates ( $x$ ) over the range of  $-1 \text{ in.} \leq x \leq 1 \text{ in.}$ . For each coordinate the step size was 0.5-inch. The magnet center is defined to be at  $(z, x) = 0 \text{ in.}, 0 \text{ in.}$ . Data from this mapping are given in table 14.

Data in table 14 indicates that on the mid-plane the (vertical) rms field is reasonably uniform over a region 2 inches wide centered on the centerline. The difference from the field on the centerline and that 1 inch on either side varies from  $\sim 3\%$  at the extremes of the measurements, where the fields are to  $\sim 3 \text{ G}$ , to  $\sim 0.3\%$  at the magnet center, where they are  $\sim 136 \text{ G}$ .

Also listed in table 14 are the calculated  $\int B \cdot dz$  and the effective length  $L_{eff}$  along each of the longitudinal traverses. The reference value for the  $\int B \cdot dz$  (that measured along the centerline) was  $\int B_{rms}(z, 0) dz = 1,546.15 \text{ G}\cdot\text{in.}$  In the calculation of  $L_{eff}$  the field at the magnet center was used for normalization:  $B_{rms,norm} = B_{rms}(0, 0) = 135.9 \text{ G}$ .

The average value of the calculated effective lengths is

$$\langle L_{eff} \rangle = \frac{11.3333 + 11.3672 + 11.3771 + 11.3635 + 11.3653}{5} = 11.3613 \text{ in.} = 0.28858 \text{ m},$$

which is  $\sim 3\%$  shorter than the dc measurements. The largest difference between this average value and a calculated value of  $L_{eff}$  is  $-0.028 \text{ inch}$ , or  $-0.25\%$ , along the  $x = -1 \text{ inch}$  line. This constancy of  $\int B \cdot dz$

and of  $L_{eff}$  is also indicative of the uniformity of the field of the magnet.

Figure 7 is a composite plot of the field variation along each (longitudinal) traverse. In order to show the falloff of the fields from their central values each traverse for  $x \geq -0.5$  inch is shifted 0.5 inch upstream of the data for its downstream neighbor. It is seen that the measurements for each traverse are similar.

#### 4. Implications for use of these steering magnets in beam line 2A

This study has shown that an rms field of  $\sim 136$  G can be produced at the specified maximum rms current of 3.5 A. Assuming that we may adequately estimate the peak field from  $B_{peak} = \sqrt{2} B_{rms}$ , this means that the maximum peak field to be expected is  $\sim 192$  G. To calculate the expected deflection  $\theta$  of the beam at this value of peak field we proceed as follows. Because small angle ( $\sim 2$  mr) deflections are required we may assume that the arc length  $s (= \rho\theta)$  of the trajectory in a magnet is equal to the effective length of the magnet. Then because

$$B(\text{kG})\rho(\text{m}) = 33.356 p(\text{GeV}/c) ,$$

we have

$$\begin{aligned} 33.356 p(\text{GeV}/c) &= B(\text{kG})\rho(\text{m}) \\ &= B(\text{kG}) \frac{s(\text{m})}{\theta} \\ &= B(\text{kG}) \frac{L_{eff}(\text{m})}{\theta} . \end{aligned}$$

Thus the expected deflection is

$$\theta(\text{radian}) = \frac{B(\text{kG})L_{eff}(\text{m})}{33.356 p(\text{GeV}/c)} .$$

Using the values calculated above of  $\langle L_{eff} \rangle = 0.28858$  m and  $B_{peak} = 192$  G together with the momentum  $p$  of a 500 MeV proton ( $1.09007$  GeV/c), we find that the maximum deflection expected per magnet is

$$\theta_{max} = \frac{(0.192 \text{ kG})(0.28858 \text{ m})}{33.356(1.09007 \text{ GeV}/c)} = 1.52 \text{ mr} .$$

Consequently, for two magnets in series the maximum total deflection of the beam in either the horizontal or vertical planes is expected to be

$$\theta_{max,total} = 2(1.524 \text{ mr}) = 3.05 \text{ mr} .$$

#### 5. Discussion

This report has presented the results of ac magnetic measurements of the four ANAC steering magnets that are proposed to be installed (eventually) in beam line 2A for the production of an annular beam spot at the east and west targets of the line. These results have shown that these magnets would be suitable for that purpose and, in particular, that they can be used at frequencies at or below 20 Hz with the existing power supplies. It is also indicated that given upgraded supplies, the magnets should be capable of operating at frequencies in the range of 100–110 Hz.

The  $B_{rms}$ – $I_{rms}$  results given in tables 2–5 indicate that the four magnets are quite similar in both the horizontal and vertical planes. Indeed, a generic fit to all of the measured data in each plane fits the measured fields to better than 1% except at currents below 1 A. That separate fits were required for each of the horizontal and vertical planes is indicative of a slight difference of the horizontal and vertical coils of each magnet. For three of the four magnets (#11, #13 and #14) the horizontal coil requires a slightly higher voltage to produce a given current and therefore a given field. For magnet #9, however, this is

reversed; it is the vertical coil that requires the higher voltage.

The field plots shown in figure 7 show that the field is uniform over a region that is  $\pm 3$  inches about the longitudinal centerline and  $\pm 1$  inch about the transverse centerline. The fall-off of the field from its value in the center of the magnet is also shown to be virtually identical over the region measured.

#### *References*

1. G. M. Stinson, *On the production of a hollow beam spot at the beam line 2A target*, TRIUMF Report TRI-DNA-00-2, TRIUMF, June, 2000.
2. D. Evans, *Private communication*, TRIUMF, July, 2006.
3. J. L. Chuma, *PHYSICA USER'S GUIDE*, TRIUMF Report TRI-CD-98-01, TRIUMF, February, 1998.

Table 1. Measurements on the vertical coil of magnet #14.

$I_{rms}$ (A)	$B_{dc}$ (G)	$V_{dc}$ (V)	$B_{rms}$ (G)	$V_{rms}$ (V)	$B_{peak}$ (G)
0.5	19.7	1.6	19.0	2.1	27
1.0	38.4	3.3	37.0	4.3	54
1.5	56.8	5.0	56.4	5.9	80
2.0	75.5	6.7	75.5	8.0	110
2.5	94.1	8.4	95.2	10.0	140
3.0	112.9	10.1	114.8	12.0	162
3.5	131.8	11.8	134.3	14.1	190

Table 2. Measurements on the coils of magnet #9.

$I_{rms}$ (A)	$B_{rms,vert}$ (G)	$V_{rms,vert}$ (V)	$B_{rms,hor}$ (G)	$V_{rms,hor}$ (V)
0.5	17.3	2.23	17.4	2.14
1.0	36.4	4.49	36.5	4.30
1.5	55.8	6.75	56.0	6.47
2.0	75.4	9.02	75.6	8.64
2.5	95.1	11.30	95.4	10.83
3.0	114.6	13.60	115.0	13.03
3.5	134.3	15.90	134.7	15.25

Table 3. Measurements on the coils of magnet #11.

$I_{rms}$ (A)	$B_{rms,vert}$ (G)	$V_{rms,vert}$ (V)	$B_{rms,hor}$ (G)	$V_{rms,hor}$ (V)
0.5	17.5	1.93	17.4	2.02
1.0	36.6	3.87	36.7	4.00
1.5	56.2	5.83	56.2	6.02
2.0	76.0	7.78	75.8	8.03
2.5	95.4	9.75	95.5	10.06
3.0	115.3	11.73	115.2	11.10
3.5	135.1	13.71	134.9	14.15

Table 4. Measurements on the coils of magnet #13.

$I_{rms}$ (A)	$B_{rms,vert}$ (G)	$V_{rms,vert}$ (V)	$B_{rms,hor}$ (G)	$V_{rms,hor}$ (V)
0.5	17.5	1.92	17.5	2.00
1.0	36.6	3.86	36.6	4.00
1.5	56.2	5.81	56.1	6.01
2.0	75.8	7.77	75.6	8.03
2.5	95.5	9.73	95.4	10.07
3.0	115.1	11.70	115.0	12.10
3.5	134.9	13.69	134.8	14.16

Table 5. Measurements on the coils of magnet #14.

$I_{rms}$ (A)	$B_{rms,vert}$ (G)	$V_{rms,vert}$ (V)	$B_{rms,hor}$ (G)	$V_{rms,hor}$ (V)
0.5	17.5	1.96	17.4	2.02
1.0	36.6	3.93	36.4	4.03
1.5	56.2	5.90	55.8	6.06
2.0	75.7	7.89	75.5	8.10
2.5	95.5	9.88	95.0	10.14
3.0	115.2	11.89	114.6	12.20
3.5	134.8	13.90	134.4	14.26

Table 6. Coefficients  $\alpha$  and  $\beta$  in linear fits to individual  $B_{rms,meas}-I_{rms}$  measurements

Magnet	Vertical		Horizontal	
	$\alpha$ (G/A)	$\beta$ (G)	$\alpha$ (G/A)	$\beta$ (G)
#9	39.05	-2.54285714	39.1642857	-2.52857143
#11	39.2428571	-2.47142857	39.20	-2.44285714
#13	39.1785714	-2.41428571	39.1428571	-2.42857143
#14	39.1714286	-2.41428571	39.0428571	-2.500
Average	39.1716071	-2.40671428	39.1375000	-2.475

Table 7. Measured and fitted values in the vertical plane of  $B_{rms}$  as a function of  $I_{rms}$  <sup>†</sup>

Magnet	$I_{rms}$ (A)	$B_{rms,meas}$ (G)	$B_{rms,fit}$ (G)	$B_{rms,diff}$ (%)
#9	0.5	17.3	17.12	1.043
	1.0	36.4	36.70	-0.824
	1.5	55.8	56.28	-0.861
	2.0	75.4	75.86	-0.611
	2.5	95.1	95.44	-0.359
	3.0	114.6	115.02	-0.368
	3.5	134.3	134.60	-0.225
#11	0.5	17.5	17.12	2.173
	1.0	36.6	36.70	-0.273
	1.5	56.2	56.28	-0.143
	2.0	76.0	75.86	-0.183
	2.5	95.4	95.44	-0.431
	3.0	114.6	115.02	-0.368
	3.5	134.3	134.60	-0.225
#13	0.5	17.5	17.12	2.173
	1.0	36.6	36.70	-0.273
	1.5	56.2	56.28	-0.143
	2.0	75.8	75.86	-0.080
	2.5	95.5	95.44	0.062
	3.0	115.1	115.02	0.068
	3.5	134.9	134.60	0.221
#14	0.5	17.5	17.12	2.173
	1.0	36.6	36.70	-0.273
	1.5	56.2	56.28	-0.143
	2.0	75.7	75.86	-0.212
	2.5	95.5	95.44	0.062
	3.0	115.2	115.02	0.155
	3.5	134.8	134.60	0.147

<sup>†</sup>  $B_{rms,fit}$  was obtained from the fit to *overall* vertical data:

$$B_{vert,rms,meas}(\text{G}) = 39.1607143 I_{rms}(\text{A}) - 2.46071429$$

Table 8. Measured and fitted values in the horizontal plane of  $B_{rms}$  as a function of  $I_{rms}$  <sup>†</sup>

Magnet	$I_{rms}$ (A)	$B_{rms,meas}$ (G)	$B_{rms,fit}$ (G)	$B_{rms,diff}$ (%)
#9	0.5	17.4	17.09	1.760
	1.0	36.5	36.66	-0.445
	1.5	56.0	56.23	-0.413
	2.0	75.6	75.80	-0.265
	2.5	95.4	95.37	0.033
	3.0	115.0	114.94	0.054
	3.5	134.7	134.54	0.144
#11	0.5	17.4	17.09	1.760
	1.0	36.7	36.66	0.102
	1.5	56.2	56.23	-0.056
	2.0	75.8	75.80	0.0
	2.5	95.5	95.37	0.137
	3.0	115.2	114.98	0.279
	3.5	134.9	134.51	0.292
#13	0.5	17.5	17.09	2.321
	1.0	36.6	36.66	-0.171
	1.5	56.1	56.23	-0.234
	2.0	75.6	75.80	-0.265
	2.5	95.4	95.37	0.033
	3.0	115.0	114.94	0.054
	3.5	134.8	134.51	0.218
#14	0.5	17.4	17.09	1.760
	1.0	36.4	36.66	-0.721
	1.5	55.8	56.23	-0.773
	2.0	75.5	75.80	-0.397
	2.5	95.0	95.37	-0.388
	3.0	114.6	114.96	-0.295
	3.5	134.4	134.51	-0.079

<sup>†</sup>  $B_{rms,fit}$  was obtained from the fit to *overall* horizontal data:

$$B_{hor,rms,meas}(\text{G}) = 39.1375 I_{rms}(\text{A}) - 2.475$$

Table 9. Frequency response measurements on the coils of magnet #9.

$f$ (Hz)	$B_{rms,vert}$ (G)	$V_{rms,vert}$ (V)	$B_{rms,hor}$ (G)	$V_{rms,hor}$ (V)
7*	137	15.0	137	15.0
8*	135	15.2	136	15.1
9*	135	15.5	135	15.3
10	135.0	15.79	135.0	15.36
12	134	16.50	134.2	15.83
14	134	17.32	134.0	16.46
16	133.8	18.24	134.0	17.23
18	133.5	19.25	134.1	18.11
20	133.3	20.27	133.7	18.85
22	133.3	21.40	133.7	19.71
24	133.2	22.53	133.3	20.63

\* Amplifier unstable at this frequency.

Table 10. Frequency response measurements on the coils of magnet #13<sup>†</sup>.

$f$ (Hz)	$B_{rms,vert}$ (G)	$V_{rms,vert}$ (V)	$B_{rms,hor}$ (G)	$V_{rms,hor}$ (V)
7*	136	13.0		13.3
8*	136	13.2		13.5
9*	136	13.4		13.9
10	135.5	13.70		14.22
12	134.4	14.29		14.97
14	134.4	15.01		15.84
16	134.2	15.79		16.80
18	133.9	16.63		17.83
20	134.0	17.56		18.88
22	133.7	18.49		19.99
24	133.8	19.47		21.19

<sup>†</sup>  $B_{rms,hor}$  was not measured because it was not changing.

\* Amplifier unstable at this frequency.

Table 11. Extended frequency-response measurements on the coils of magnet #13.

$f$ (Hz)	$B_{rms,vert}$ (G)	$V_{rms,vert}$ (V)	$B_{rms,hor}$ (G)	$V_{rms,hor}$ (V)
20	134	17.45	134	18.76
24	134	19.39	134	21.08
28	134	21.39	134	23.54
32	134	23.58	134	26.08
36	133.5	25.71	133.5	28.58
40	133.5	28.15	133.5	31.30
44	133.5	30.28	133.5	34.00
48	133.5	32.79	133.5	36.75
52	133.5	35.13		
56	133.5	37.66		

Table 12. Heating tests on the horizontal coil of magnet #13<sup>†</sup>.

Time (hr)	$V_{rms}$ (V) at 10 Hz	$V_{rms}$ (V) at 20 Hz
0	14.00	18.73
1	14.52	19.11
2	14.66	19.19
3	14.72	19.25
4	14.75	19.30
5	14.80	19.30
6	14.82	19.30
7	14.85	19.31
8	14.85	19.33

<sup>†</sup> At 10 Hz the coil temperature was 22.0°C at  $t = 0$  and 40.5°C after  $t = 8$  hr. Corresponding temperatures for the 20 Hz test were 21.3°C at  $t = 0$  and 40.0°C after  $t = 8$  hr.

Table 13. Measured vertical and horizontal fields along the axis of magnet #9 at an rms current of 3.5 A and a frequency of 10 Hz.

$z$ (in.)	$B_{rms,vert}$ (G)	$B_{rms,hor}$ (G)	$z$ (in.)	$B_{rms,vert}$ (G)	$B_{rms,hor}$ (G)
-10.0	2.9	2.9	0.5	134.5	134.8
-9.5	3.6	3.3	1.0	134.5	134.8
-9.0	4.8	4.4	1.5	134.4	134.8
-8.5	6.7	6.1	2.0	134.2	134.5
-8.0	9.7	9.0	2.5	133.5	133.9
-7.5	14.3	13.5	3.0	132.4	133.1
-7.0	21.1	20.3	3.5	129.3	130.4
-6.5	31.0	30.2	4.0	121.8	123.9
-6.0	45.0	44.0	4.5	106.9	110.9
-5.5	63.4	62.2	5.0	85.6	90.9
-5.0	85.5	83.9	5.5	63.9	69.0
-4.5	106.6	104.8	6.0	45.3	49.5
-4.0	121.4	120.4	6.5	31.3	34.4
-3.5	129.1	129.0	7.0	21.4	23.2
-3.0	132.4	132.6	7.5	14.6	15.5
-2.5	133.8	133.9	8.0	9.9	10.4
-2.0	134.3	134.3	8.5	6.9	7.0
-1.5	134.3	134.5	9.0	4.9	4.9
-1.0	134.5	134.6	9.5	3.6	3.7
-0.5	134.5	134.6	10.0	2.9	3.0
0.0	134.5	134.7			

Table 14. Mid-plane vertical fields in the of magnet #13 with  $I_{rms} = 3.5$  A and  $f = 10$  Hz.

$z$ (in.)	$B_{rms,vert}$ (G) at $x$ (in.) =				
	-1.0	-0.5	0.0	0.5	1.0
-10.00	3.2	3.3	3.3	3.3	3.2
-9.50	3.8	3.8	4.0	3.9	3.8
-9.00	4.9	5.0	5.2	5.1	4.8
-8.50	6.6	7.0	7.1	7.0	6.6
-8.00	9.4	9.9	0.1	9.9	9.3
-7.50	13.6	14.4	14.7	14.3	13.4
-7.00	19.9	21.2	21.6	21.1	19.7
-6.50	29.3	30.9	31.5	30.8	28.9
-6.00	42.6	44.7	45.4	44.5	42.2
-5.50	60.8	62.9	63.6	62.8	60.6
-5.00	84.2	85.0	85.3	85.1	84.5
-4.50	108.8	106.8	106.5	107.3	110.2
-4.00	125.3	122.6	122.1	123.1	126.7
-3.50	131.9	130.6	130.4	130.9	132.9
-3.00	134.3	133.9	133.9	134.0	134.9
-2.50	135.0	135.0	135.2	135.2	135.6
-2.00	135.3	135.5	135.7	135.6	135.8
-1.50	135.4	135.7	135.8	135.7	136.0
-1.00	135.5	135.8	135.9	135.8	136.0
-0.50	135.5	135.8	135.9	135.8	136.0
0.00	135.5	135.9	135.9	135.8	136.0
0.50	135.5	135.9	135.9	135.8	136.0
1.00	135.5	135.9	135.9	135.8	136.0
1.50	135.5	135.8	135.8	135.7	135.9
2.00	135.4	135.7	135.7	135.6	135.8
2.50	135.2	135.4	135.3	135.3	135.6
3.00	134.6	134.5	134.3	134.5	135.1
3.50	133.0	132.1	131.7	132.2	133.7
4.00	128.1	125.9	125.1	126.2	129.5
4.50	115.1	112.5	111.7	112.8	116.7
5.00	91.7	91.6	91.4	91.5	91.8
5.50	67.1	68.9	69.2	68.4	66.5
6.00	47.2	49.1	49.5	48.7	46.4
6.50	32.4	34.1	34.4	33.7	31.7
7.00	22.0	23.2	23.5	22.9	21.4
7.50	14.9	15.8	16.0	15.5	14.4
8.00	10.2	10.7	10.8	10.5	9.8
8.50	7.0	7.4	7.5	7.3	6.8
9.00	5.2	5.3	5.4	5.2	5.0
9.50	3.9	4.1	4.1	4.0	3.9
10.00	3.4	3.3	3.3	3.3	3.2
$\int Bdz$ (G-in.)	1,540.2	1,544.8	1,546.2	1,544.3	1,544.6
$L_{eff}$ (in.)	11.3333	11.3672	11.3771	11.3635	11.3653

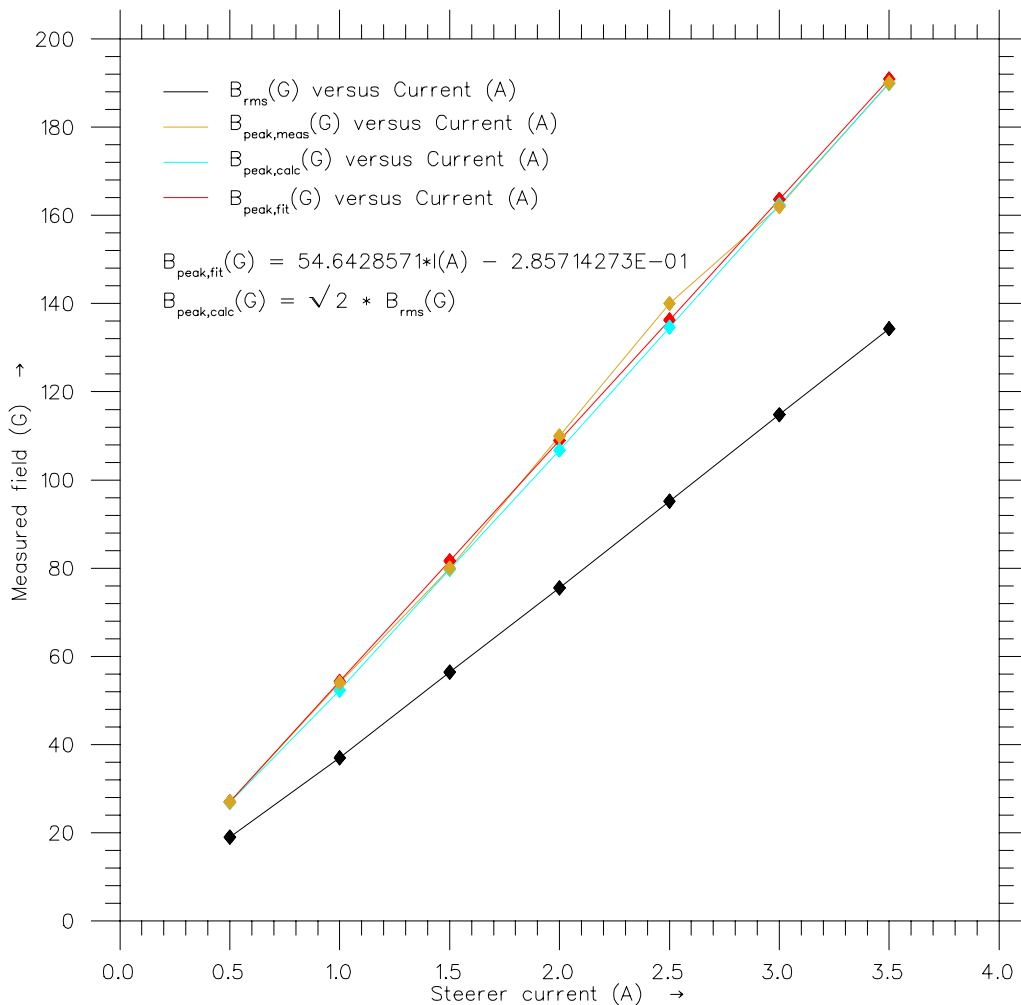


Fig. 1. Measured  $B_{peak}$  and  $B_{rms}$  data for one coil of magnet #14 at a frequency of 10 Hz.

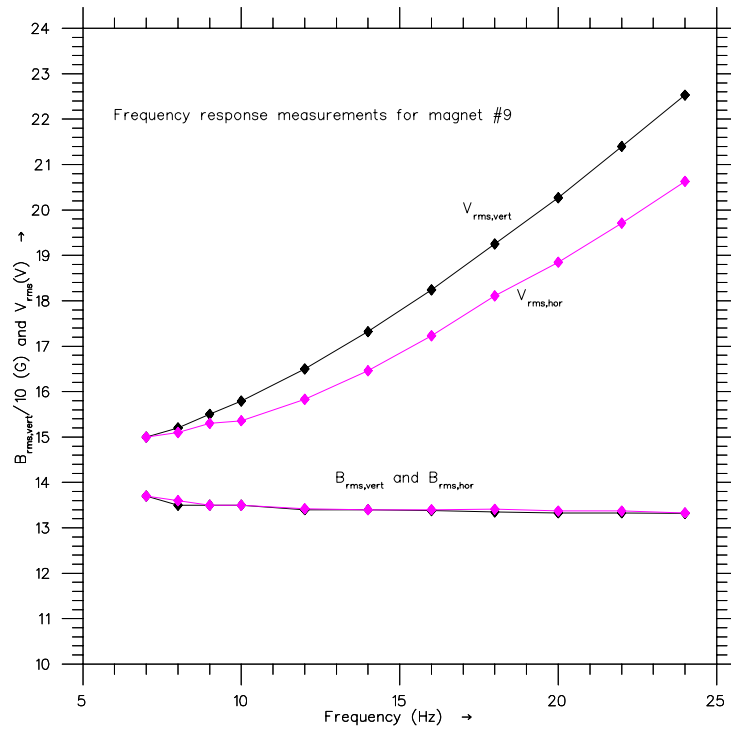


Fig. 2. Measured  $B_{rms,vert}$ ,  $B_{rms,hor}$ ,  $V_{rms,vert}$  and  $V_{rms,hor}$  as a function of frequency for magnet #9.

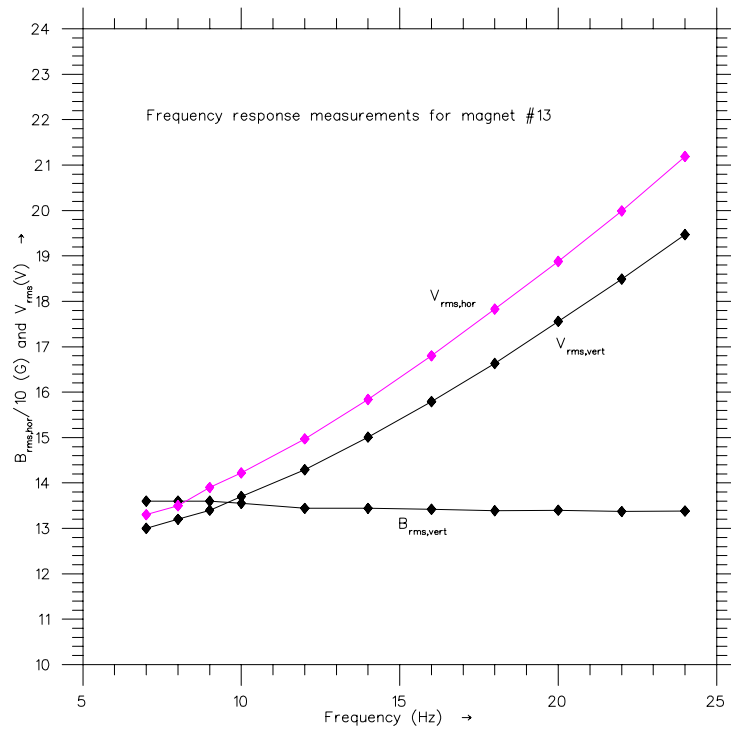


Fig. 3. Measured  $B_{rms,vert}$ ,  $V_{rms,vert}$  and  $V_{rms,hor}$  as a function of frequency for magnet #13.  $B_{rms,hor}$  was not recorded because it was the same as  $B_{rms,vert}$ .

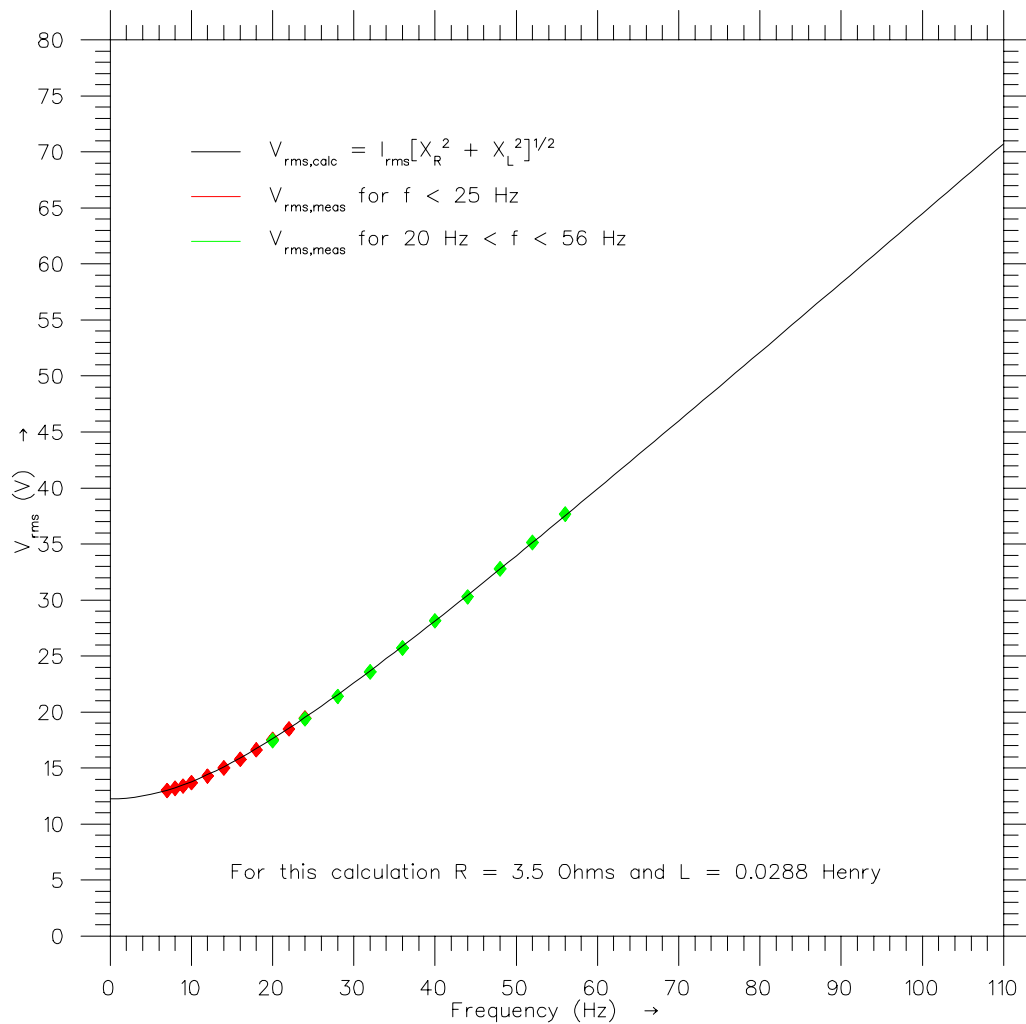


Fig. 4. Calculated and measured values of  $V_{rms}$  over a frequency range from 0 Hz to 110 Hz. Data points are those measurements from 10–25 Hz and 20–54 Hz.

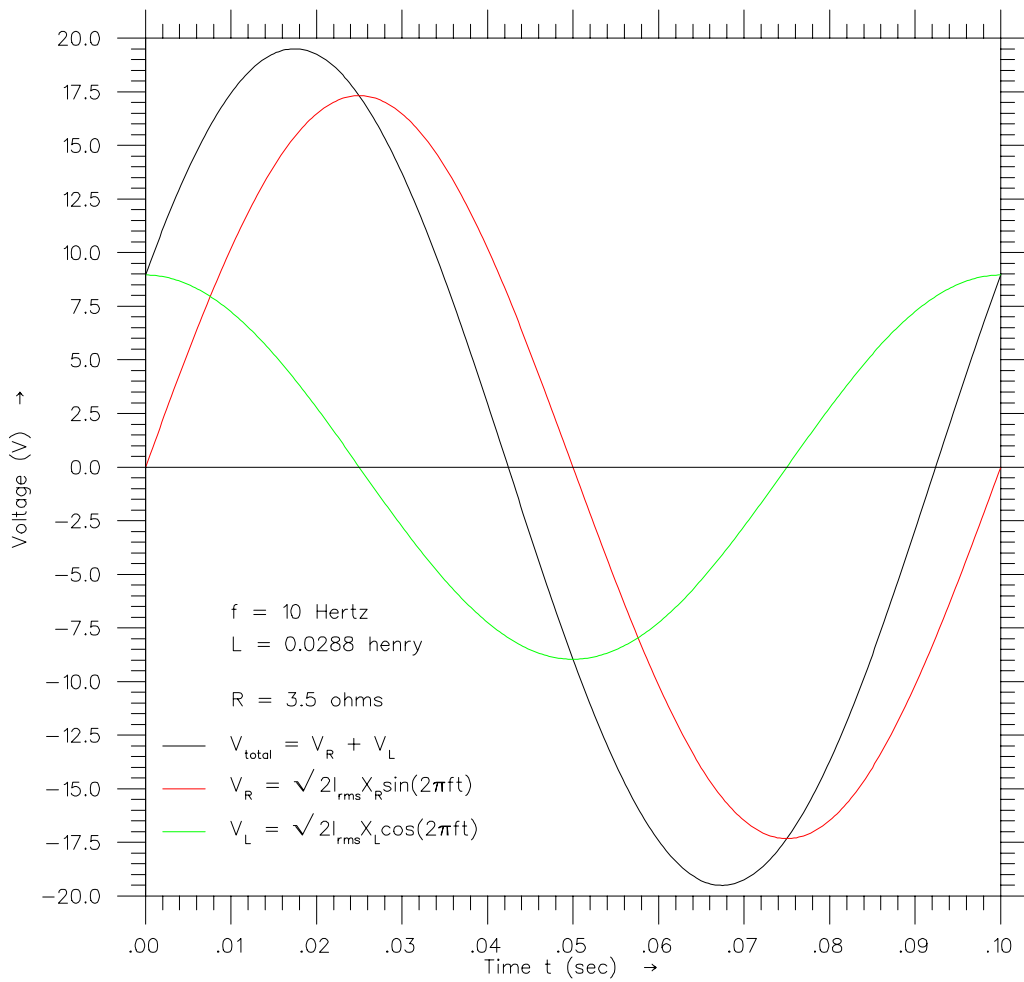


Fig. 5. Voltage waveforms over one period across the resistive and inductive components and their sum.

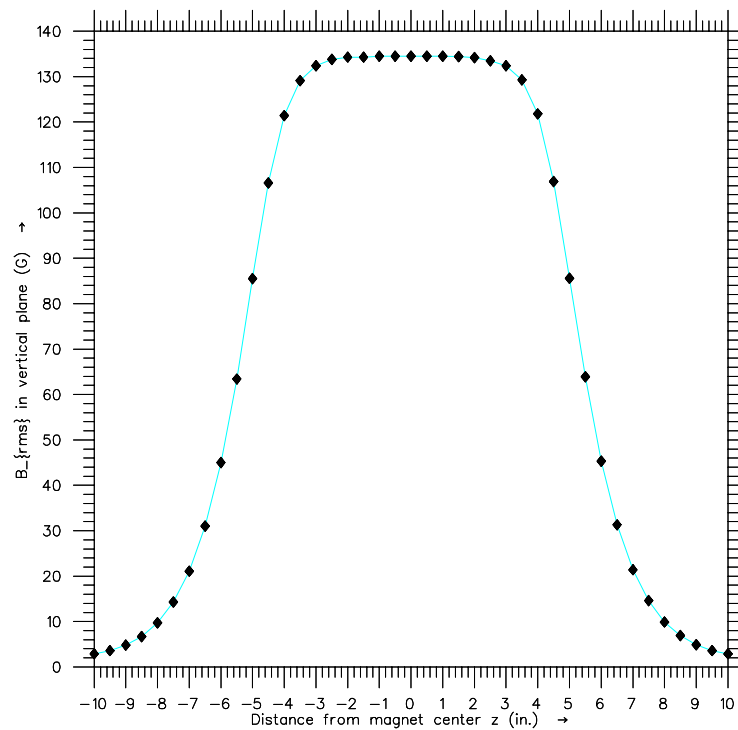


Fig. 6(a). Measured  $B_{rms}$  along the axis of magnet #9 in the vertical plane at an rms current of 3.5 A.

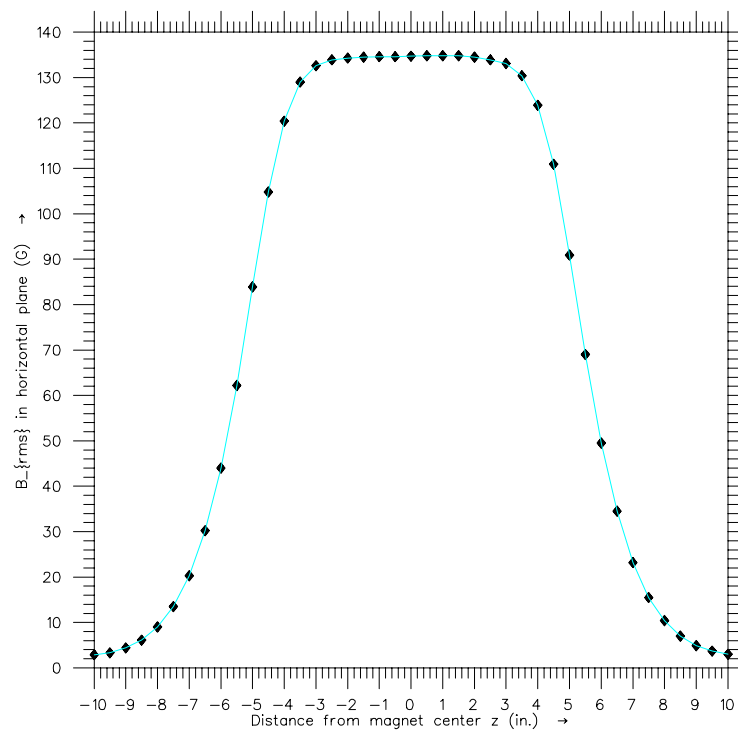


Fig. 6(b). Measured  $B_{rms}$  along the axis of magnet #9 in the horizontal plane at an rms current of 3.5 A.

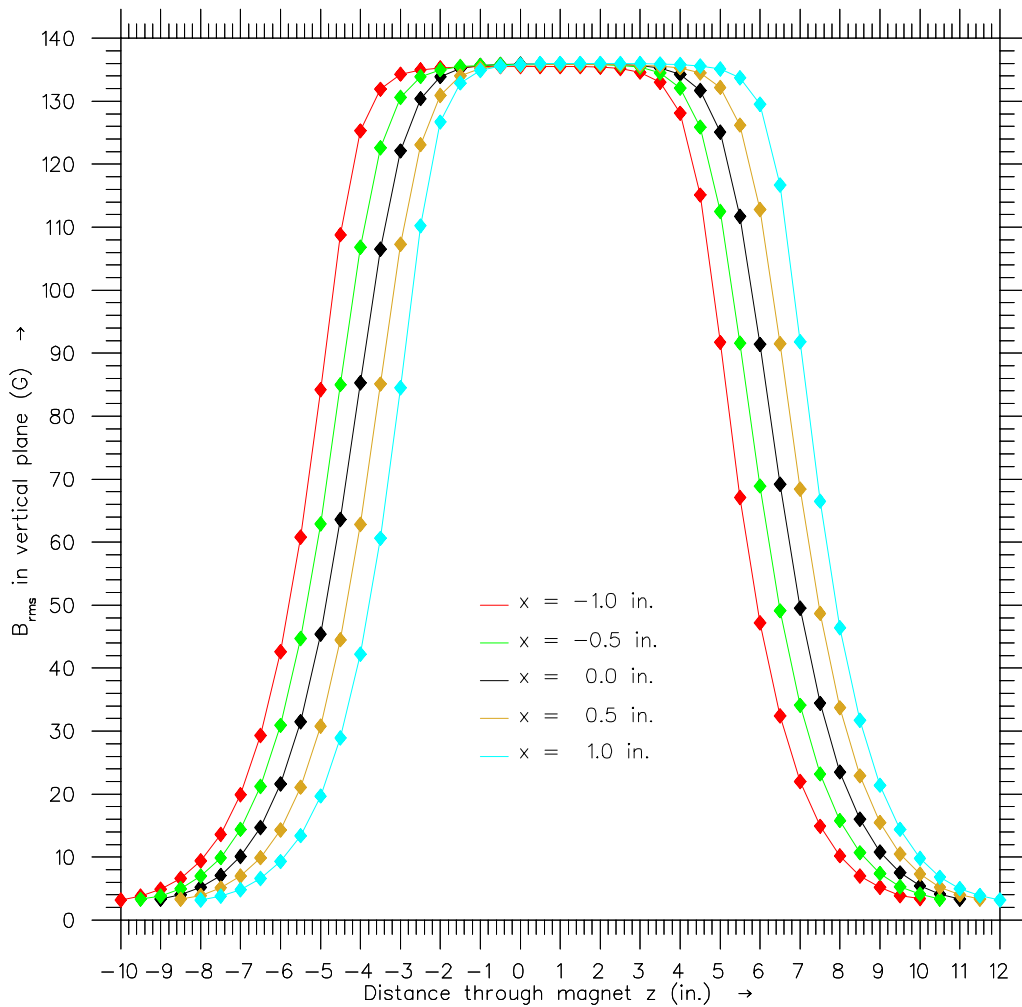


Fig. 7. Vertical  $B_{rms}$  fields on the mid-plane of magnet #13 measured along the centerline ( $x$ ) and  $\pm 1.0$  inch and  $\pm 0.5$  inch either side. Data for each traverse for  $x \geq -0.5$  inch is shifted 0.5 inch upstream (in the positive  $z$  direction) relative to its downstream neighbor in order to show the falloff from the central fields. The magnet current was 3.5 A rms and the frequency was 10 Hz for all measurements.